Article Identifier
DOI: 10.22032/dbt.58842
URN: urn:nbn:de:gbv:ilm1-2023isc-008:8

60th ILMENAU SCIENTIFIC COLLOQUIUM
Technische Universität Ilmenau, 4 – 8 September 2023
URN: urn:nbn:de:gbv:ilm1-2023isc:1

HIGH-RESOLUTION ABSOLUTE RANGE SENSORS BASED ON THE COMBINATION OF FREQUENCY MODULATION AND LASER TRIANGULATION FOR HEAVY INDUSTRY APPLICATION

Michael Krauhausen[1], Roland Priem[1], Ralf Claßen[1], Günther Prellinger[2], Florian Pollinger[2]

[1]VOLAS GmbH, Krantzstraße 7, 52070 Aachen, Germany
[2]Physikalisch-Technische Bundesanstalt (PTB), Bundesallee 100, 38116 Braunschweig, Germany

ABSTRACT

Feedback control of metal strip rolling processes requires inline-capable, fast and robust thickness gauges. An optical thickness gauge is developed which measures the distance to the top and bottom of the strip with two optical sensors. They combine triangulation and multi-wavelength interferometry for a robust absolute high-resolution range measurement. Sinusoidal modulation interferometry is used to realize a very compact Fizeau-type multi-wavelength interferometer. The performance of the thickness gauge is studied in the laboratory under dynamic conditions that are close to production environment. The expanded measurement uncertainty of 0.48 µm of the system is thereby consistent with the observed deviation of the measurement values from a tactile reference sensor.

Index Terms **–** thickness gauge, distance sensor, 2f/3f interferometry, sinusoidal modulation interferometry, multi-wavelength interferometry, laser triangulation, measurement uncertainty

1. INTRODUCTION

Thin metal foils of thicknesses between five and several hundreds of micrometres play an important role in many industrial applications, in particular to produce modern high-performance accumulators. Their production requires constant inline control and feedback during the rolling process. Respective gauges are usually installed before and after the rolling mill. Table 1 summarizes state-of-the art strip thickness measurement techniques.
To reduce the achievable uncertainties further, interferometry might seem a promising distance measurement approach. However, the difficult measurement environment poses severe challenges to be overcome for a real-life capable sensor. In a rolling mill, the strip is moving at high transport speeds of several hundred metres per minute. The thickness gauge must hence provide reliable thickness values at a high measurement rate if the signal is to be used for feedback control. Furthermore, the system must deal with vertical oscillations of several hundreds of micrometers with frequencies up to more than 250 Hz. Simple counting interferometry most certainly fails under these conditions. The optical set up, on the other hand, may not be too complex to avoid inevitable thermal drifts in the industrial environment. Finally, traceability to the SI definition of the meter is to be ensured for such a measurement of high economic relevance.

© 2023 by the authors. – Licensee Technische Universität Ilmenau, Deutschland.

This is an Open Access article distributed under the terms of the Creative Commons Attribution ShareAlike-4.0 International License, (https://creativecommons.org/licenses/by-sa/4.0/).

Table 1: State of the art measuring methods to measure strip thickness.

Method	Description	Accuracy	Advantages	Disadvantages
tactile	Probes with a specially crowned diamond tip touch the top and bottom side of the strip. The movement of the mechanical measuring inserts is recorded by inductive displacement transducers. Without strip, the probes touch each other, and the system performs an automatic zero adjustment.	0.1% related to the strip thickness to be measured, not better than 1 µm	In practice, the tactile systems are still the systems that reliably guarantee the highest measurement accuracy. The devices are robust against strip vibrations and moisture on the belt as well as fog at the location of measurement.	Sometimes tactile probes leave scratch marks on sensitive surfaces (e.g., tinned strip). Probes wear out and must be replaced periodically. Probes heat up during measurement. The devices are prone to thermal drift.
x-ray	The thickness is indirectly determined via absorption of radiation. The absorption depends on the material.	0.1% related to the strip thickness to be measured, not better than 0.5 µm	Very robust and insensitive to environmental influences, can also be used in hot rolling mills.	No direct measurement of the thickness. Alloy must be known for accurate measurement. Not applicable to composite materials. Costly safety measures due to x-ray radiation.
laser triangu-lation	Laser triangulation sensors measure the distance to the top and bottom of the strip. The distance between the sensors is determined via a calibration routine by measuring gauge blocks. The strip thickness can be determined contact free. There is no dependence on the material alloy.	Not better than 1 µm. In most cases > 2 µm.	Non-contact measurement that works regardless of the alloy of the material.	The windows of the sensors must be protected against contamination by additional technology. The roughness of the surface influences the measurement result. The devices are prone to thermal drift. The linearity errors of the sensors require that the pass line is kept as constant as possible. No reliable measurement when the strip is not moving.
confocal chromatic	Chromatic aberration of white light is used to derive the distance to top and bottom of the strip.	Not better than 0.5 µm.	Non-contact measurement that works regardless of the alloy of the material.	Linearity error of 0.5×10^{-6} of the measuring range. Thermal drift of the sensors of approx. 2 µm/K, considerably larger than other optical techniques [1].
pulsed eddy current (PEC)	The technology is based on the measurement of the voltage pulse induced in the coil when the constant excitation current is suddenly interrupted. It is an indirect measurement of thickness.	Not better than 1 µm	Very robust and insensitive to environmental influences.	Only applicable for non-ferrous metals; not applicable for ferrous alloys. The material to be measured must have a minimum thickness of approx. 0.02 mm. The large measuring area makes measurement at the strip edge and with narrow strips (< 250 mm) difficult.

© 2023 by the authors. – Licensee Technische Universität Ilmenau, Deutschland.

In this study, an optical sensor system is developed that pushes the uncertainty limit well below 1 µm. The distance measurement is realized by a combination of triangulation and multi-wavelength interferometry [2]. A very compact optical sensor design is achieved using 2f-3f-interferometry [3] and fast inline data processing ensured by a strict implementation of the analysis in Field Programmable Gate Arrays (FPGA). The combination of mechanical design and on-site calibration with gauge blocks provides the necessary robustness against the challenging environment. In the following, the measurement method is introduced, and the system design discussed in detail. Verification measurements using a production simulator experiment are presented and the major uncertainty contributions are discussed.

2. MEASUREMENT PRINCIPLE

Surface roughness and vibrations make it practically impossible to track the thickness of a metal strip under rolling mill conditions by conventional counting interferometry due to the small range of non-ambiguity. When a distance is measured by two or more interferometers of different wavelengths λ_i (i=1, 2, …), however, the additional information can be used to extend the non-ambiguity range by several orders of magnitude [4-7]. In case of two-wavelength interferometry, this new ambiguity range is given by half of the synthetic wavelength

$$\widetilde{\Lambda}_s = \frac{\lambda_1 \cdot \lambda_2}{\lambda_1 - \lambda_2}. \qquad (1)$$

In air, the vacuum wavelength $\widetilde{\Lambda}_s$ is reduced by the two-colour group refractive index n_g. It can be derived from the phase refractive n_i by

$$n_\mathrm{g} \equiv n_1 - \frac{n_1 - n_2}{\lambda_1 - \lambda_2}\lambda_1. \quad (2)$$

Since the system is calibrated in air during its initialization procedure (cf. Section 3), the synthetic wavelength in air $\Lambda_\mathrm{s} \equiv \widetilde{\Lambda}_\mathrm{s}/n_\mathrm{g}$ is consistently worked with in the following. The phase difference $\Delta\phi$ between the optical phase difference ϕ_1 and ϕ_2 is referred to as the synthetic phase ϕ_s. If a coarse pre-value l_pre for the absolute distance is known, the absolute geometric path difference l in a multi-wavelength interferometer can be calculated by [8-10]

$$l = \left[\mathrm{floor}\left(\frac{l_\mathrm{pre}}{\Lambda_\mathrm{s}/2} - \frac{\phi_\mathrm{s}}{2\pi} + \frac{1}{2}\right) + \frac{\phi_s}{2\pi}\right] \times \frac{\Lambda_s}{2} \quad (3)$$

with floor(x) representing the next integer value z with $z \leq x$. The uncertainty of the coarse pre-value l_pre only needs to better than $\Lambda_\mathrm{s}/4$. In the online thickness sensor, the coarse value is to be determined continuously in parallel by the triangulation sensor.

If two or more interferometers are to be measured in parallel, their signals need to be disentangled for the analysis. For this purpose, it is beneficial to modulate the frequency ν of the laser sources periodically by the modulation index $\Delta\nu$ with the modulation frequency f_m, so that the emitted light frequency ν is the given by

$$\nu = \nu_0 + \Delta\nu \sin(\omega_m t) \qquad (4)$$

with $\omega_m = 2\pi f_m$. The intensity I detected by the receiver of an interferometer of path length difference Δz can then described by [10]

$$\mathrm{I} = I_0[1 + \cos(\phi_0 + \Delta\phi \sin(\omega_m t))] \qquad (5)$$

© 2023 by the authors. – Licensee Technische Universität Ilmenau, Deutschland.

where $\Delta\phi$ denotes the amplitude of the phase modulation and ϕ_0 the classical interferometer phase of interest

$$\Delta\phi = 4\pi\frac{\Delta\nu\Delta z n}{c} \qquad (6)$$

$$\phi_0 = \mathrm{mod}\left(4\pi\frac{n\Delta z}{\lambda}, 2\pi\right) \qquad (7)$$

with c representing the vacuum speed of light and n the phase refractive index. To derive the targeted interference phase ϕ_0 from the complex system, there are multiple sophisticated approaches [11-15]. Using Bessel functions J_i ($i = 0, 1, 2, \ldots$), Equation (5) can be developed into the following series expansion [3]:

$$I = I_0\begin{bmatrix}1 + J_0(\Delta\phi)\cos(\phi_0) - 2J_1(\Delta\phi)\sin(\omega_\mathrm{m}t)\sin(\phi_0) \\ +2J_2(\Delta\phi)\cos(2\omega_\mathrm{m}t)\cos(\phi_0) - 2J_3(\Delta\phi)\sin(3\omega_\mathrm{m}t)\sin(\phi_0) + \ldots\end{bmatrix}. \qquad (8)$$

In Eq. (6), the free parameter modulation index $\Delta\nu$ can be chosen so that the condition

$$J_2(\Delta\phi) = J_3(\Delta\phi) \qquad (9)$$

is fulfilled. The optical phase can then by retrieved according to [3]:

$$\phi_0 = \arctan\left[\frac{I(3f_\mathrm{m})}{I(2f_\mathrm{m})}\right] = \arctan\left[\frac{\sin(\phi_0)}{\cos(\phi_0)}\right]. \qquad (10)$$

This analysis approach is sometimes referred to as 2f-3f-interferometry. A special advantage is the fact that a full retrieval of the optical phase can be achieved without the need of additional optics or phase shifting lock-in techniques.

3. EXPERIMENTAL

Figure 1 gives an overview of the design of the thickness gauge. Its main component is a C-shaped rigid frame (A) with two optical sensors (C) measuring the distance to the top and bottom side of the part under test, e. g. a running metal foil (B). The C-frame is made from Invar ($\alpha_T \cong 1.5\times10^{-6}$ / K). Figure 2 shows the mechanical setup of the thickness gauge. The frame can be moved horizontally and vertically via two linear slides with stepper motors. This allows scanning of stationary targets, especially a tray with four gauge blocks which are used for adjustments and as thickness reference. A separate control unit contains the light sources, beam splitters, and most of the electronics for detection and data reduction. It is connected to the frame via optical single mode fibers (one per interferometer) and an ethernet connection.

Two tunable DFB laser diodes with nominal wavelengths of 795 nm and 780 nm are used as light sources for the interferometers. According to Eq. (1), their joint analysis corresponds to a synthetic wavelength Λ_s of approximately 41.817 µm. For the unwrapping according to Eq. (3) to work, the uncertainty of the coarse measurement should not exceed one fourth of the synthetic wavelength [10]. For a measuring range of 4 mm, a measurement uncertainty of 10 µm can be typically achieved by a triangulation measurement. The coarse pre-value for the

© 2023 by the authors. – Licensee Technische Universität Ilmenau, Deutschland.

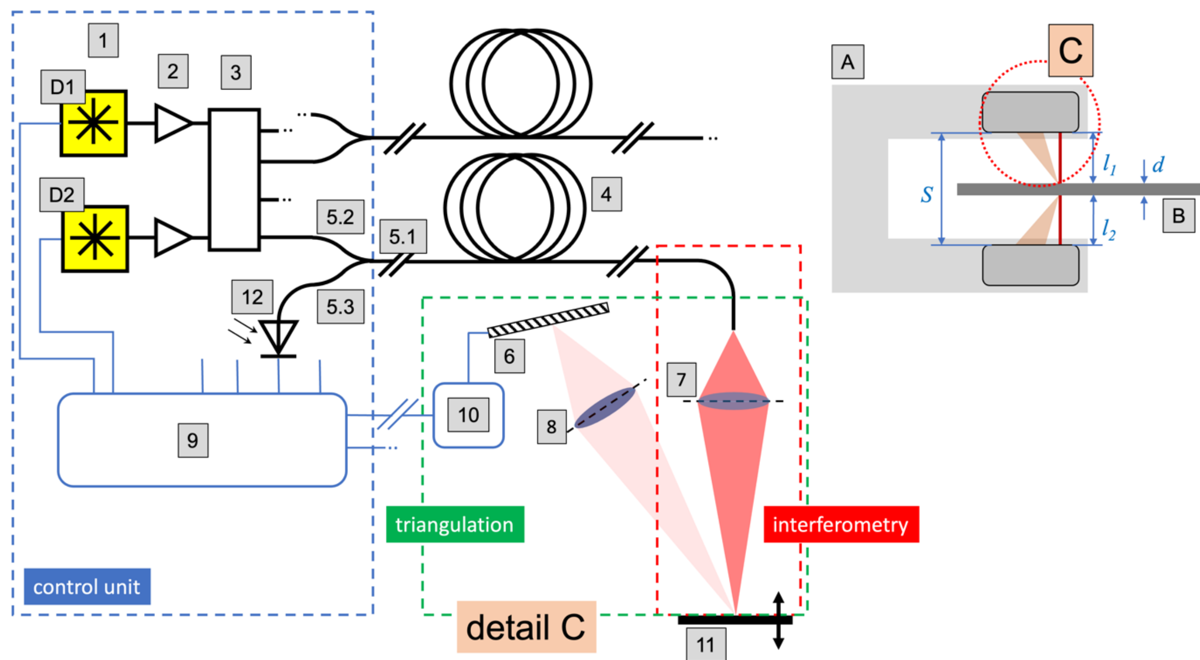

Figure 1: A: Thickness gauge; B: metal strip; C: optical sensor; Detail C: Sketch of the design of the interferometric distance sensor used in the thickness gauge, D1/D2 DFB diodes. The absolute distance can be derived by combination of the phase values of the interferometer and the distance information of the triangulation part of the sensor. 1: DFB laser diode; 2: optical isolator; 3: 2-4 fiber splitter; 4: single mode fiber; 5:Y-fiber splitter; 5.3: photo diode; 6: CMOS line detector; 7: focusing lens; 8: image lens; 9: controller; 10: triangulation readout FPGA, 11: metal strip, 12: photo diode.

interferometric length measurement can hence be determined by triangulation. Each diode is enclosed in a butterfly housing with fiber output that also includes a thermoelectric cooler and a thermistor for temperature control and an optical isolator (2) to prevent small mode hops induced by back-reflected light. Following the scheme of Figure 1, the light from the two diodes is first combined into a single fiber and then split into four fiber outputs (3), each passing its light through a Y-coupler (ports 5.2 and 5.1) to an interferometer (7). A Si PIN photo diode (bandwidth ≈ 100 MHz) placed at the third port of the Y-coupler (5.3) observes the light that comes back from the interferometer. Two of these channels are used for the distance sensors, the other two are available for expansion. To measure the distance via triangulation, a second lens (8) observes the light diffusely scattered by the target under an angle of ≈ 30° and projects it onto a CMOS linear image sensor (6) with 1024 pixels. A small FPGA (10) in each sensor continuously reads the image data with a pixel rate of 40 MHz, calculates the triangulation distance and transmits it to the control unit (9) via Ethernet. This arrangement ensures that coarse and fine measurement are taken from the same spot on the strip.
The laser diodes are modulated with sine waves of 1.2 MHz (diode 1) and 1.5 MHz (diode 2). The modulation waveforms are digitally generated by the main FPGA in the control unit with an output rate of 125 MHz, amplified and superimposed onto the DC diode current via a bias-tee circuit. The modulation amplitudes can either be adjusted in the FPGA or by varying the gains of the amplifiers. As neither the coupling characteristics of the bias-tee nor the current sensitivities of the diodes at high modulation frequencies are sufficiently known, the amplitudes must be determined once by experimentation for a given arm length difference. The modulation frequencies have been chosen so that the minimum distance between any of the first four harmonics of both sines is maximized while keeping the base frequency below 1.5 MHz.
The control unit contains four photodiode receivers. Each receiver first converts the light-induced changes to the diode current into a voltage signal with a trans impedance amplifier.

© 2023 by the authors. – Licensee Technische Universität Ilmenau, Deutschland.

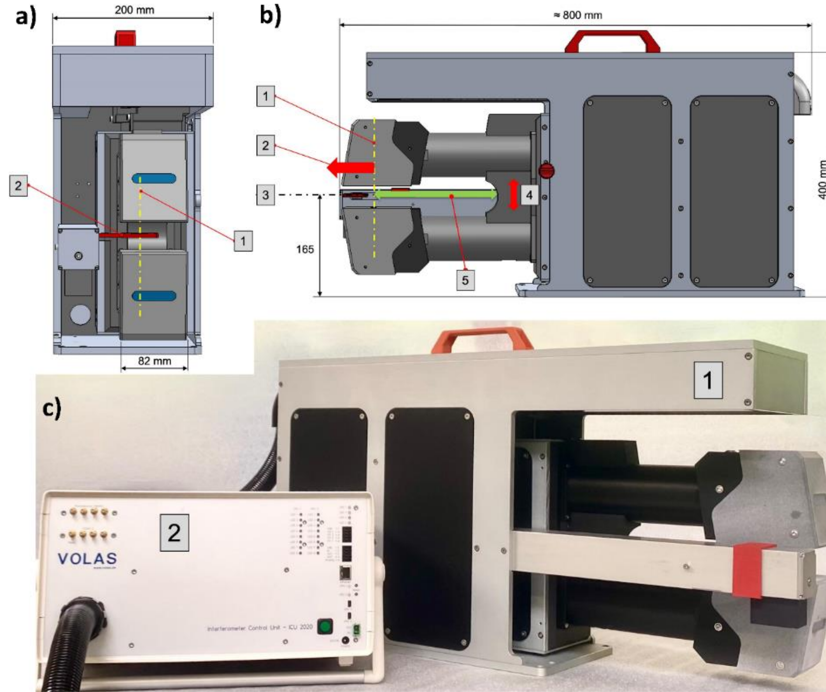

Figure 2 Full set up of the thickness sensor gauge. a) Schematic front view: 1: beam axis, 2: holder for reference gauge blocks. b) Schematic side view: 1: beam axis, 2: moveable horizontal position of the C-frame, 3: pass line (zero position), 4: moveable vertical position of the C-frame. c) prototype of the thickness gauge. 1: measurement head, 2: control unit

The voltage signal then passes through a bandpass filter that removes frequencies above approx. 40 MHz to avoid aliasing effects during digitization and dampens below approx. 2 MHz to partially suppress the strong signals from the modulation frequencies. Finally, the signal is amplified by a programmable gain factor and digitized with a sample rate of 125 MHz. A digital lock-in is realized by the FPGA. It provides an output rate of 100 kHz with a bandwidth limit of 35 kHz. Triangulation and interference data are then assigned by latency-compensated time stamps. Using the triangulation distances, the FPGA performs a distance-dependent Heydemann correction [16] on each pair of lock-in amplitudes $x = I(2f)$, $y = I(3f)$ to compensate for remnant non-linearities and inevitable unbalanced signal amplification. Figure 3 demonstrates the dependence of the nonlinearity of the sensor signal on the position of the sample within the measurement range of the sensor. Finally, the interferometric phases $\phi_{1,2}$ are calculated.
The remaining data reduction steps (deconvolution and thickness calculation) are performed on a dedicated real time processor inside the FPGA. First, the noise in the triangulation distance readings is reduced by removing obvious outliers and applying a moving average filter (window size ±30 samples, which introduces a latency of 300 µs). Each interferometric distance reading l_I is then calculated according to Eq. (3)

$$l_I = \frac{\Lambda_s}{2}\left(N_\mathrm{s} + G_0 + \frac{\phi_s}{2\pi}\right) \qquad (11)$$

using the synthetic phase ϕ_s and the synthetic wavelength Λ_s in air (cf. Eq. (3) and (4)) and the dimensionless parameter G_0 (one value per sensor) which compensates for the offset between the origin of the triangulation scale and the scale of the synthetic interferometer. The integer order N_s is calculated using the (smoothed) triangulation distance l_T as pre-value:

© 2023 by the authors. – Licensee Technische Universität Ilmenau, Deutschland.

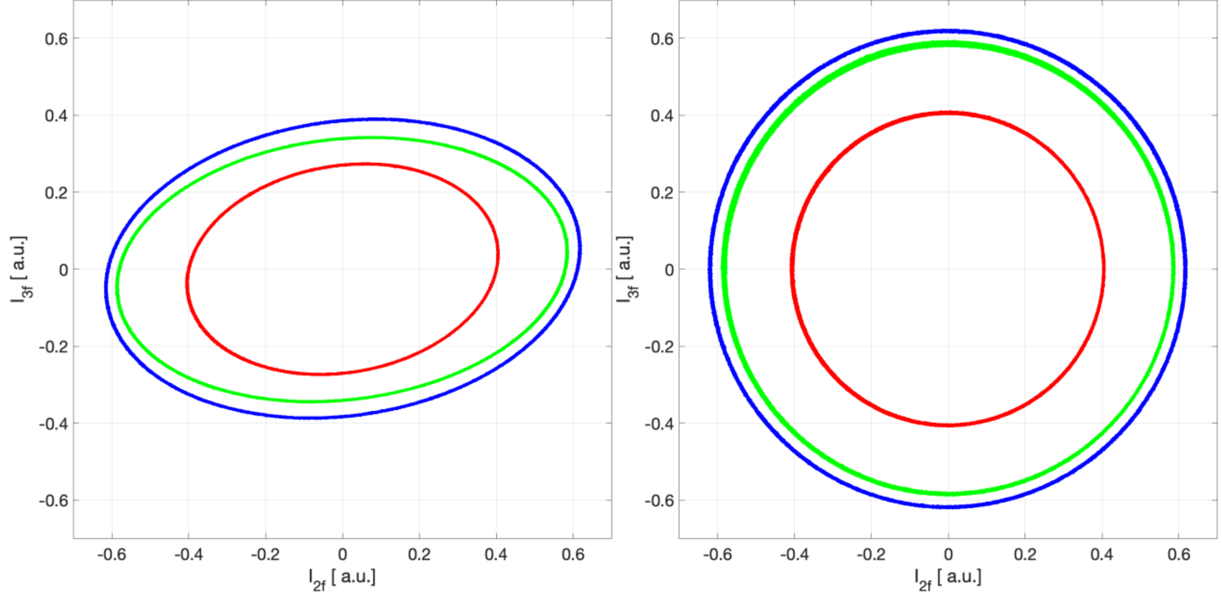

Figure 3 2f-3f data processing. Different colors correspond to different positions of the sample surface in the measurement range: green: near end, blue: center, red: far end. Left: the uncorrected data is distorted due to imperfectly balanced signal amplification and other non-linear effects. Right: after distant-dependent Heydemann correction, using parameters independently determined in the initialization procedure.

$$N_\mathrm{s} = \mathrm{floor}\left(\frac{2l_\mathrm{T}}{\Lambda_\mathrm{s}} - G_0 - \frac{\phi_\mathrm{s}}{2\pi} + \frac{1}{2}\right) \qquad (12)$$

Subtracting the sum of the two deconvoluted interferometric distances l_1 and l_2 from an adjustment constant S finally yields the thickness d:

$$d = S - (l_1 + l_2). \qquad (13)$$

A final processing step removes obvious outliers and applies a lowpass filter (typically a moving average with a time window of 10 to 100 ms). A special case of outliers are readings where the integer order N_s has been miscalculated for one sensor. As a sudden thickness change of ≈ 20 µm is not to be expected in a typical milling process, they can be corrected for by adding an appropriate integer multiple of $\Lambda_s/2$.

Four calibrated gauge blocks of nominal lengths 0.3, 0.5, 0.7, and 1.0 mm are used to derive the synthetic wavelength Λ_S in air as well as the parameters S and G_0. This initialization procedure ensures traceability of the result to the SI definition of the meter. Since it is performed on site before the actual milling process, this adjustment and calibration procedure limits the impact of the challenging production environment in heavy industry.

4. RESULTS AND DISCUSSION

The performance of the thickness gauge is studied using a simulator for the highly dynamical measurement conditions in the rolling mill. The inset of Figure 4a shows the respective setup. Start and end of a stainless-steel strip of 4.5 m length and a thickness of approximately 638 µm are welded together. This strip is mounted on two rolls which can drive it at velocities between 40 and 200 m/min. The optical thickness gauge is place in between the two rolls. As reference, a tactile thickness gauge is placed in the setup as well. Both gauges are aligned so that they measure at approximately the same distance from the strip edge. Figure 4 depicts exemplary data for a strip speed of 160 m/min. The thickness profiles are averaged over 25 revolutions

© 2023 by the authors. – Licensee Technische Universität Ilmenau, Deutschland.

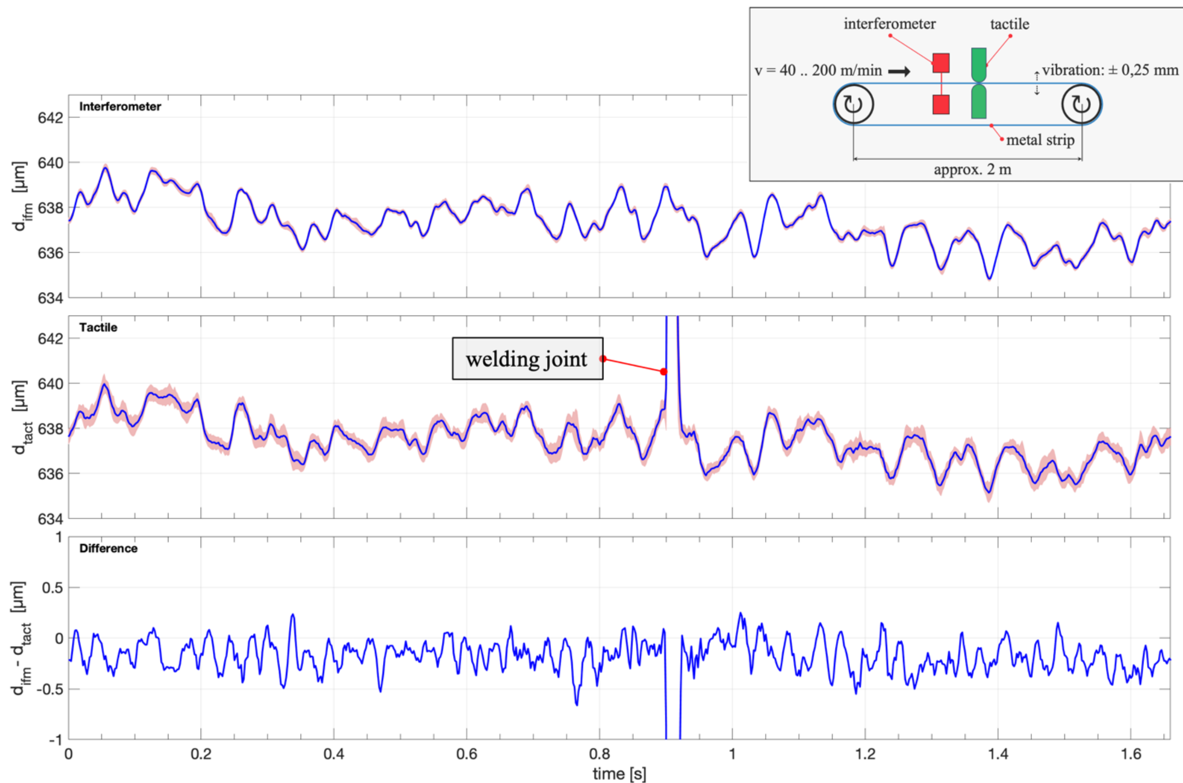

Figure 4 Comparison between interferometric and tactile strip thickness sensor. Blue lines indicate the average profile, the pink data indicates the noise of the 25 measurements. a) Strip thickness as measured by the interferometric thickness gauge at strip velocity of 160 m/min. Inset: experimental setup. b) thickness as deduced by a tactile measurement. c) Deviation between both measurements

using an autocorrelation algorithm. Lateral shifts due to the different gauge positions are compensated. The qualitative features from optical (Figure 4a) and tactile (Figure 4b) gauges agree well. The noise in the tactile data (indicated in pink in Figure 4b) is considerably larger than in the case of the optical measurement (pink data in Figure 4a). The difference between the two averaged curves shows an overall offset. The tactile gauge seems to measure a systematically thicker strip in the order of 200 nm. Several effects can contribute to the observed offset. For once, the measurement position might not have coincided well enough. There is additional experimental evidence that the thickness of the reference sample varies over the strip width in the order of a few hundred nanometers. Furthermore, the techniques have different sensitivities. On an imperfect, rough surface, a finite tactile probe will not be able to map the full depth, while the optical signal contains reflections from the complete surface. But thermal drifts within the two gauges cannot be ruled out either.

Respective experiments have been performed for different strip velocities between 40 and 200 m/min. The results are summarized in Figure 5. The deviation of the mean values shown in lower part of Figure 5 indicates the optical and tactile thickness measurement to deviate by a maximum value of $\Delta d_{\text{max}} = 0.30$ µm. The range R of the strip thickness is systematically larger for the tactile than for the interferometric gauge (cf. upper part of Figure 5). Again, there are several explanations. The non-contact optical measurement is probably less sensitive to mechanical oscillations. Furthermore, the optical probe averages the signal over the full beam width, while the mechanical probe is sensitive to the most prominent extrusions of the surface roughness.

Table 2 summarizes the uncertainty contributions to the presented interferometric strip thickness gauge under typical production environments and provides their weight to the overall expanded measurement uncertainty. The full discussion and derivation of the uncertainty bud-

© 2023 by the authors. – Licensee Technische Universität Ilmenau, Deutschland.

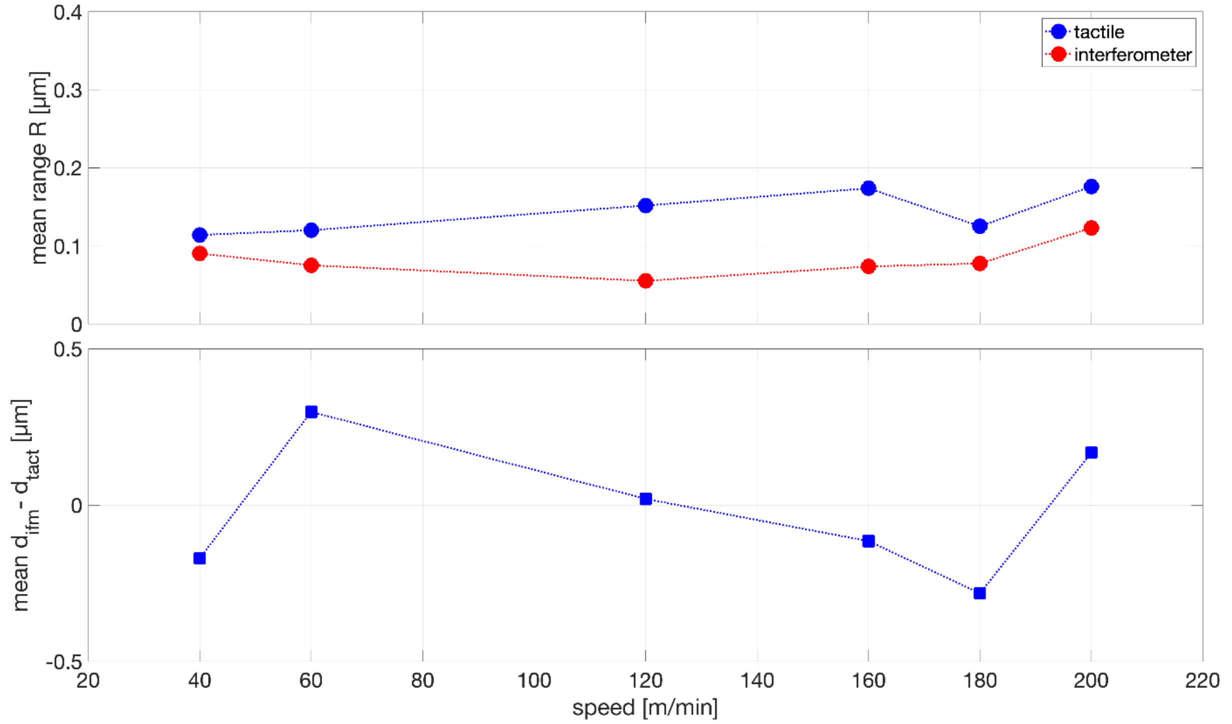

Figure 5: Comparison of tactile and interferometer measurements at different strip speeds. The upper graph indicates the mean range of the thickness values measured at identical spots for the 25 strip revolutions. The lower graph depicts the mean deviation between the thickness measurements of interferometric and tactile gauge.

get will be presented elsewhere [17]. According to the "Guide to the expression of Uncertainty in Measurement" (GUM) [18], an expanded measurement uncertainty $U = 0.48$ µm is derived. The predominant contributions are changes in the two-colour group index of refraction during the measurement (weight 18.3 %) and the thermal expansion of the C-mount (75.9 %). Both contributions are assessed assuming a controlled operation in a quasi-steady state environment. The temperature, in particular, is expected to remain within ±2.0 K after the initial calibration of the gauge. Changes in the index of refraction are reduced by a constant air flow introduced into the measurement volume [19]. Despite the use of low-thermal expansion material for the C-frame design, the associated thermal expansion remains the dominating uncertainty contribution. Therefore, additional constructive measures like a temperature control of the C-frame are being considered.
The comparison measurement between interferometric and tactile gauge can be used to verify the derived measurement uncertainty. The accuracy of the tactile gauge is given by the manufacturer by approximately 1.0 µm for the strip thicknesses below 1 mm. Lacking further specification, a coverage factor of k=2 is assumed. The $k = 1$ combined uncertainty of the reference value provided by the tactile measurement is hence estimated to $u_{\mathrm{ref}} = 0.50$ µm. For the observed maximum deviation of $\Delta d_{\max} = 0.30$ µm between the completely independent measurement values of the interferometric and tactile sensor, the degree of equivalence can be calculated by [20]

$$E_n = \frac{\Delta d_{\max}}{2\sqrt{u_{ref}^2 + u_{comb}^2}} = 0.27 < 1.0. \qquad (14)$$

A degree of equivalence smaller than 1.0 supports the assumed measurement uncertainties [20]. While further verification experiments against other reference systems given in Table 1 are yet

© 2023 by the authors. – Licensee Technische Universität Ilmenau, Deutschland.

Table 2 Measurement uncertainty budget for the metal strip thickness measurement [17].

Uncertainty contribution		standard uncertainty / µm	weight
gauge resolution	u_{res}	0.0029	0,01%
thermal expansion reference gauge block	$u_{\Delta T,\mathrm{gb}}$	0.0054	0,05%
bias (against external reference gauge blocks)	u_{bias}	0.0346	2,11%
standard deviation thickness gauge alone	$u_{\sigma,\mathrm{g}}$	0.0320	1,80%
vacuum wavelength stability	u_{λ}	0.0176	0,54%
index of refraction	u_{ng}	0.1021	18,31%
equipment variation	u_{EV}	0.0268	1,26%
thermal expansion metal strip	$u_{\Delta T,\mathrm{st}}$	0.0058	0,06%
thermal expansion C-frame	$u_{\Delta T,S}$	0.2078	75,86%
combined uncertainty (k=1)	u_{comb}	0.24	
expanded measurement uncertainty (k=2)	U	0.48	

to be performed, the results of this comparison experiment are hence consistent with the expanded measurement uncertainty of 0.48 µm for the interferometric thickness gauge.

5. CONCLUSIONS

An interferometric measurement in a rolling mill production environment is a highly challenging task. Modulation interferometry allows an efficient, robust and compact implementation of multi-wavelength interferometry. The combination of interferometry and triangulation has been achieved using the same optical source, ensuring that both sensors simultaneously measure at the same spot on the strip. The thickness measurement on the fast rotating and oscillating sample has been simulated by a dedicated experiment. The qualitative agreement between tactile and optical sensors is convincing. Although this quantity varies unsystematically, the observed deviations remain below 300 nm, and thus well below the practical requirements in a rolling mill. With decreasing foil thicknesses, a better understanding of the physical origin or the correct technical interpretation of these deviations is necessary. The observed deviations are well consistent with the derived expanded measurement uncertainty of 0.48 µm for the interferometric measurement. Nevertheless, further verification measurements against other methods of smaller measurement uncertainty seem desirable. Finally, it should be noted that the main uncertainty component, the thermal expansion of the C-frame, is independent from the optical measurement principle. Any gauge using two sensor top-bottom design suffers from this purely mechanical property. The expanded measurement uncertainty of 0.48 µm with all contributions is certainly already today a leading measurement capability for these types of sensors, making a convincing case for the application of interferometry even under these uncollaborative conditions.

Acknowledgments
All authors acknowledge partial funding by the German technology transfer program “TransMET”. M.K., R.P., and R.C. further acknowledge funding by the “ZIM” program under the funding identifier EP190169.

Competing financial interests
M.K., R.P., and R.C. are employees of VOLAS GmbH. VOLAS GmbH is developing the sensor system further with the target of commercialization.

© 2023 by the authors. – Licensee Technische Universität Ilmenau, Deutschland.

REFERENCES

[1] G. Berkovic, S. Zilberman and E. Shafir, “Temperature effects in chromatic confocal distance sensors”, *SENSORS, 2013 IEEE*, Baltimore, MD, USA, pp. 1-3, 2013.
[2] M. Krauhausen, R. Priem, and A. Selent. “Verfahren zur optischen Abstandsmessung sowie ein Abstandsmessgerät”. Patent DE102016100745B3. 2017.
[3] K. Meiners-Hagen, V. Burgarth, and A. Abou-Zeid, “Profilometry with a multi-wavelength diode laser interferometer”, Measurement Science and Technology 15, p. 741-746. 2004.
[4] M. R. Benoît, “Application des phénomènes d'interférence à des déterminations métrologiques”, Journal de Physique Théorique et Appliquée 7, p. 57-68, 1898.
[5] J. C. Wyant, “Testing Aspherics Using Two-Wavelength Holography”, Appl. Opt. 10, p. 2113-2118, 1971.
[6] C. Polhemus, “Two-Wavelength Interferometry”, Appl. Opt. 12, p. 2071-2074, 1973.
[7] K. Meiners-Hagen. R. Schödel. F. Pollinger. and A. Abou-Zeid. “Multi-Wavelength Interferometry for Length Measurements Using Diode Lasers”, Measurement Science Review 9, p. 16-26, 2009.
[8] P. J. de Groot, “Extending the unambiguous range of two-color interferometers”, Appl. Opt. 33, p. 5948-5953, 1994.
[9] S.-H. Lu and C.-C. Lee, “Measuring large step heights by variable synthetic wavelength interferometry”, Measurement Science and Technology 13, p. 1382-1387, 2002.
[10] F. Pollinger, K. Meiners-Hagen, M. Wedde, and A. Abou-Zeid. “Diode-laser-based high-precision absolute distance interferometer of 20 m range”, Appl. Opt. 48, p. 6188-6194, 2009.
[11] J. Zheng. “Analysis of optical frequency-modulated continuous-wave interference”, Appl. Opt. 43, p. 4189-4198, 2004.
[12] T. Suzuki, K. Kobayashi, and O. Sasaki, “Real-time displacement measurement with a two-wavelength sinusoidal phase-modulating laser diode interferometer”, Appl. Opt. 39, p. 2646-2652, 2000.
[13] T. Kissinger, T. O. H. Charrett, R. P. Tatam, “Range-resolved interferometric signal processing using sinusoidal optical frequency modulation”, Opt. Express 23, p. 9415-9431, 2015.
[14] O. Gerberding, “Deep frequency modulation interferometry”, Opt. Express 23, p. 14753-14762, 2015.
[15] K.-S. Isleif, O. Gerberding, T. S. Schwarze, M. Mehmet, G. Heinzel. and F. G. Cervantes, “Experimental demonstration of deep frequency modulation interferometry”, Opt. Express 24, p. 1676-1684. 2016.
[16] P. L. M. Heydemann, “Determination and correction of quadrature fringe measurement errors in interferometers”, Appl. Opt. 20, p. 3382-3384, 1981.
[17] M. Krauhausen, R. Priem, R. Claßen, G. Prellinger, and F. Pollinger, in preparation.
[18] “GUM: Guide to the Expression of Uncertainty in Measurement: Evaluation of measurement data”, JCGM 100:2008, 2008.
[19] A. Selent, R. Priem, H. Winkelmann, and M. Krauhausen, “Vorrichtung zur Konstanthaltung des Brechungsindexes im Messspalt”, Patent DE102015108076B4. 2018.
[20] M. G. Cox, “The evaluation of key comparison data”, Metrologia 39, p. 589 – 595, 2002.

CONTACTS

M. Krauhausen — email: michael.krauhausen@volas.de
ORCID: 0009-0003-6702-6352

R. Priem — email: roland.priem@volas.de
ORCID: 0009-0006-5654-3356

© 2023 by the authors. – Licensee Technische Universität Ilmenau, Deutschland.

R. Claßen email: ralf.classen@volas.de
G. Prellinger email: guenther.prellinger@ptb.de
ORCID: 0000-0003-4919-0258
Dr. F. Pollinger email: florian.pollinger@ptb.de
ORCID: 0000-0002-8494-4687

© 2023 by the authors. – Licensee Technische Universität Ilmenau, Deutschland.